Journal of the Korean Ceramic Society
https://doi.org/10.1007/s43207-024-00397-7

ORIGINAL ARTICLE

A comparative study on the structural, electronic, and magnetic properties of the cubic Sr-based perovskite $SrXO_3$(X = Mn, Sn, Cr): DFT calculation

O. Ramdane[1] · M. Labidi[1,2] · S. Labidi[1] · R. Masrour[3]

Received: 10 January 2024 / Revised: 3 March 2024 / Accepted: 24 March 2024

Abstract
In this work, we report detailed calculations on the structural, electronic, and magnetic properties of the $SrSnO_3$, $SrMnO_3$, and $SrCrO_3$ using the full-potential linearized augmented plane-wave (FP-LAPW) method implemented in the WIEN2K code. The three materials share the computing of the structural and the electronic properties; however, the magnetic properties were calculated only for both $SrMnO_3$ and $SrCrO_3$ where the $SrSnO_3$ is a non-magnetic material. Furthermore, our results are in good agreement with the available experimental data showing a little error difference on the structural parameters close to 0.04, 0.03, and 0.04 for the $SrMnO_3$, $SrCrO_3$, and the $SrSnO_3$, respectively.

Keywords DFT · Oxide perovskites · Structural · Electronic · Magnetic properties

1 Introduction

The perovskites play a crucial role in advanced technology and research due to their great multiple characteristics and diverse properties including superconductivity [1], mechanical [2] by working on the elastic properties [3], thermoelectric [4] by studying the thermoelectric transport properties [5], also for solar cells uses [6, 7] and optoelectronic devices in photovoltaic applications [8], ferroelectricity [9] for spintronic devices as S. Idrissi et al. proved it in their research [10] and many more. In recent decades, there has been increasing interest in understanding the fundamental perovskites because of them essential need in various modern technologies such as piezoelectricity, magneto transport, thermoelectric, giant magnetoresistance, charge ordering, and ferroelectricity [11, 12]. The general formula of perovskite materials is ABX_3, where A and B are two cations (A being larger than B) and X stands for an anion. Perovskites encompasses a family of materials sharing the same atomic arrangement. The anions can include oxide, sulfide, bromide, chloride, fluoride, or hydride. Notably, perovskites phases hold significance in ternary systems characterized by the ABX_3 with often oxygen serving as the anion (X) and we call them oxide perovskites. And the modification of these elements (A, B, X) and their substitutions by others leads make a deep change in their intrinsic properties which opens a huge field and research. Recent studies have focused on calculating the structural, electronic, magnetic, and elastic properties of oxides perovskites based on strontium $SrKO_3$ (K = Mn, Fe, Co, Tc, Ru, Rh, Re, Os, and Ir) and cubic $SrAO_3$ (A = Ca, Ge). These I investigations aim to demonstrate their physical stability, ferro/antiferromagnetic behavior, and thermoelectric properties as indicated in references [13, 14]. In the present work, we intend to study three perovskites having the common chemical composition ($SrXO_3$) (X = Mn, Sr, Cr) in detail by investigating their structural stability as well as electronic and magnetic properties. And this is attributed to the fact that there has been very little or no research work so far on the materials we choose. Therefore, we are motivated by these reasons to conduct these calculations, aiming to provides reference data

✉ M. Labidi
m.labidi@ensti-annaba.dz

✉ R. Masrour
rachidmasrour@hotmail.com

[1] LNCTS Laboratory, Department of Physics, Faculty of Sciences, Badji Mokhtar University, Annaba, Algeria

[2] National Higher School of Technology and Engineering-Annaba, Annaba, Algeria

[3] Laboratory of Solid Physics, Faculty of Sciences Dhar El Mahraz, Sidi Mohamed Ben Abdellah University, BP 1796, Fez, Morocco

Published online: 22 April 2024

for experimentalists and complete the existing theoretical studies on these materials. To this end, we employed the ab-initio method from the density-functional theory (DFT) implemented in the WIEN2K code.

2 Theory

In the current study, the calculations were carried out using the full-potential linearized augmented plane-wave (FP-LAPW) [15] method based on the density-functional theory (DFT) [16, 17] as implemented in the WIEN2k code [18]. The considered $SrXO_3$ perovskites are assumed to have ideal cubic structure (Pm-3m) (space group (no. 221)) with experimental cubic parameters equal to $a = 3.86$ Å [19], $a = 4.0713$ Å [20], and $a = 3.82$ Å [21] for the $SrMnO_3$, $SrSnO_3$, and $SrCrO_3$, respectively. The unit cells of our compounds are illustrated in Fig. 1 with the atomistic positions following Wyckoff positions as tabulated in Table 1 was used to study all selected perovskite oxides in this work. Where the values of muffin tin sphere radii RMT used for Sr, Sn, Mn, Cr, and O are chosen as 2.49, 1.99, 1.89, 1.83, and 1.72 (a.u), respectively. The exchange–correlation term is treated with the generalized gradient approximation GGA–PBEsol [22] to solve the Kohn–Sham equation [23]. Solution of the equation was used to study the structural, electronic, and magnetic properties of $SrXO_3$ (X = Mn, Sn and Cr) perovskite compounds. Also, to investigate the electronic properties, we used the modified Becke–Johnson GGA (mBJ- GGA) [24, 25] to correct the calculation of the GGA, because it is often underestimating the band gap. $R_{mt} \times K_{max}$ of 8.0 was used, where R_{mt} is the smallest of the atomic sphere radii and Kmax is the plane-wave cut-off wave vector. The maximum angular momentum, ℓ, was set to 10 with G_{max} equal to 12. The k-point integration over the Brillouin zone is performed using the tetrahedral method [26] and conducted with mesh with 500 kgen points, where 1000 kgen points for a mesh were used for the density of state's calculations. The self-consistent calculations were carried out with a total energy convergence tolerance of less than 0.1 mRy.

Table 1 Atomic positions in simple cubic oxide perovskite crystal

Site	Location	Coordination
A-cation (Sr)	(2a)	(0,0,0)
B-cation (Mn, Cr, Sn)	(2a)	(0.5,0.5,0.5)
O-cation (O)	(6b)	(0.5,0.5,0) (0.5,0,0.5) (0,0.5,0.5)

3 Results and discussion

3.1 Structural properties

The current study investigates the structural properties and geometries of the strontium-based perovskites $SrSnO_3$, $SrCrO_3$, and $SrMnO_3$ in both ferromagnetic and non-magnetic states using the GGA-08 approximation. Mn-3d

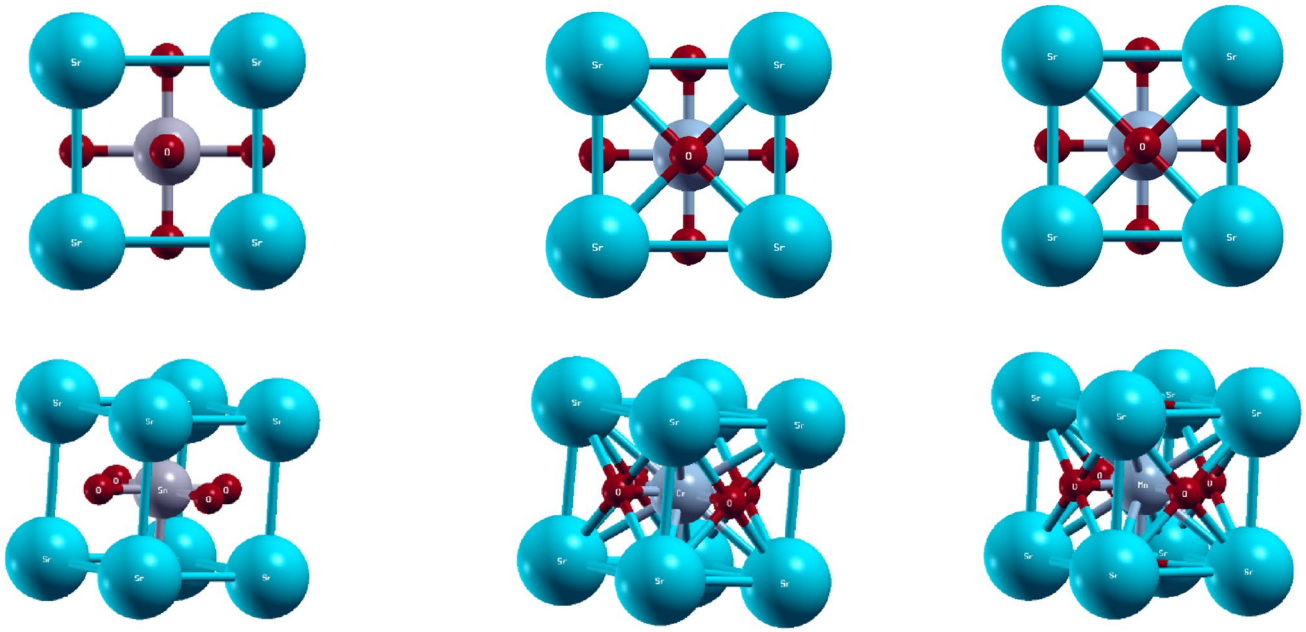

Fig. 1 Cubic simple structure (Pm3m) for the perovskites $SrSnO_3$, $SrCrO_3$, and $SrMnO_3$

orbitals in compound. $Sr(Cr,Mn)O_3$ perovskites are responsible for the ferromagnetic behavior [27, 28]. The $SrSnO_3$ is non-magnetic perovskite [29]. Figure 1 illustrates the atomic positions in the primitive cell of the crystal lattice and shows that the unit cell of every perovskite contains five atoms in a single formula unit based on the Wyckoff positions shows in Table 1 for Pm3m group. The Sn, Cr, and Mn atoms occupy the centered position of the cube, and the Sr atoms occupy the corner positions, while the O atoms occupy the face centered positions. For a description of geometric structure as mentioned earlier, the calculated total energies versus volumes are plotted and fitted to the Murnaghan's equation of state (1) [30]

$$E_{tot}(V) = E_0 + \frac{BV}{B'(B'-1)}\left\{\left(1-\frac{V_0}{V}\right) + \left(\frac{V_0}{V}\right)^{B'} - 1\right\}. \quad (1)$$

To calculate the bulk modulus (B), the pressure derivative of bulk modulus (B′), and the total energy $E_{0,}$ where V_0 is the equilibrium volume at which E_{tot} becomes minimal.

The plots of the calculated total energies versus reduced volume for all the compounds in both states are given in Fig. 2; those plots help to determine the ground state of our perovskites, i.e., when the energy resulting from all interactions between electrons and ions in the studied systems was the lowest. After observation, we notice that both of the $SrMnO_3$ and the $SrCrO_3$ are ferromagnetic materials where the $SrSnO_3$ is a non-magnetic material. On the other hand, the optimization gives also the equilibrium lattice constants a_0, the bulk modulus B_0 and its first-order pressure derivative B', the cell equilibrium volumes V_0, and the total energies which are given in Table 2.

Our calculated values of lattice constants are in good agreement with the available previous studies, as shown in Table 2 [31–36]. The results show that the lattice

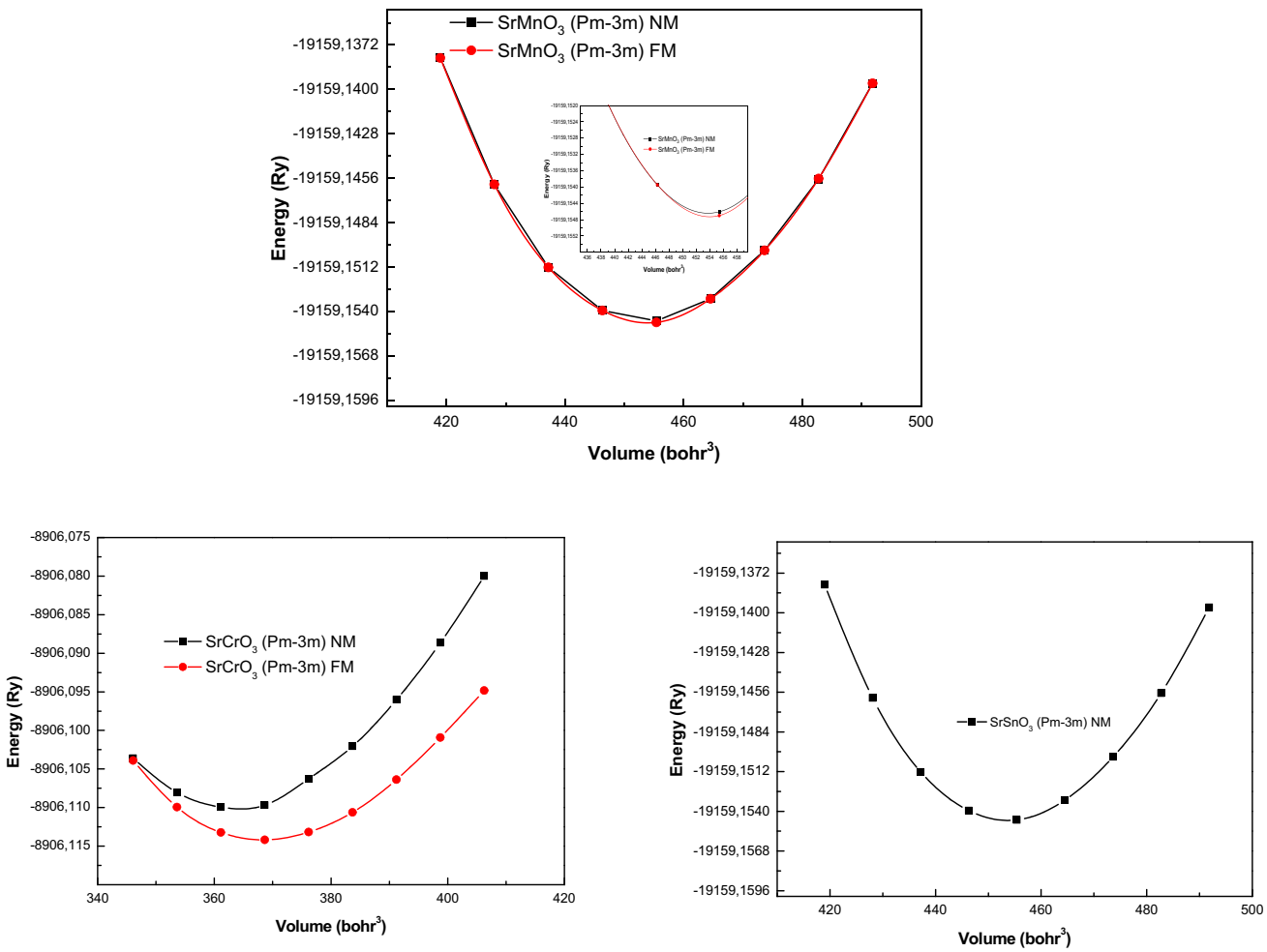

Fig. 2 Total energy per atom as function of volume for $SrXO_3$ compounds (X = Mn, Cr and Sn)

Table 2 Calculated Lattice constants, bulk modulus, bulk modulus derivatives, ground-state energies, formation energies, and equilibrium volumes of the studied compounds

Parameter	State		Compounds		
			$SrMnO_3$	$SrCrO_3$	$SrSnO_3$
	FM	Our work	3.7939	3.7932	–
	NM		3.7553	3.7739	4.0656
		Other cal	3.806 [31]	3.820 [31]	4.030 [32]
		Exp	3.800 [34]	3.811 [35]	4.025 [33]
Equilibrium volume ($Å^3$)	FM	Our work	54.60	54.57	–
	NM		52.95	53.74	67.20
		Other cal ($Å^3$)	55.13[31]	55.74[31]	–
		Exp	–	–	–
Bulk modulus (GPa)	FM	Our work	196.3816	189.4780	–
	NM		213.3463	221.4911	158.6619
		Other cal	201.7525[36]	–	167.69[32]
		Exp	–	–	–
Bulk modulus derivative	FM	Our work	5.9735	7.2411	–
	NM		5.6223	6.5350	4.8417
		Other cal	10.4377[36]	–	–
		Exp	–	–	–
Total energy (Ry)	FM	Our work	− 9121.44496691	− 8906.09483275	
			− 9121.37183749	− 8906.08001073	–
	NM	Other cal	–	–	− 19,159.1396194
		Exp	–	–	–
Formation energies E_f (Ry)	FM	Our work	− 2.07256491	− 5.49683273	–
	NM		− 2.72842049	− 2.49693473	− 2.334538
		Other cal	–	–	–
		Exp	–	–	–

parameter of SrMnO3 ≈ $SrCrO_3$ < $SrSnO_3$, and this can be referred to the increasing of the atomic size from Mn to Sn atoms as we go right the group of the periodic table. Taking into consideration the FM stable states, in $SrMnO_3$, the lattice constants are 1.17%, overestimated by GGA approach and in $SrCrO_3$ are 0.97% over estimated, while 1% underestimated for the $SrSO_3$. These results show the reliability of our calculated values and can be used as input variables for further studies without any hesitation. The calculated total energies of the stated compounds in addition to the formation energies listed in Table 2 show that $E_f(SrCrO_3) < E_f(SrMnO_3) < E_f(SrSnO_3)$. Hence, $SrCrO_3$ is the most stable among the three compounds. The computed energy values were found to be negative, reflecting the binding energy between atoms. It has been also remarked that the FM phase has minimum energy, suggesting a ferromagnetic ground state for those perovskites. The calculated bulk modulus decreases from $SrMnO_3$ to $SrSnO_3$, indicating that $SrSnO_3$ compound is harder and less compressible than the other compounds in the group. To the best of our knowledge, there are no experimental or theoretical results in the previous work for the bulk modulus and their pressure derivatives for the three studied perovskites.

3.2 Electronic properties

The obtained ground states varied with lattice parameters from optimization curve are used to calculate self-consistent in electronic properties of the perovskites. Therefore, we used the GGA– PBE and the mBJ–GGA approximations with and without spin polarization to analyze and discuss the band structures and the total and partial density of states of $SrXO_3$ (X = Mn, Cr, Sn). The density of states and the electronic band structure provide sufficient information for the characterization of the electronic properties of any material.

Figures 3 and 4 illustrate the electronic band structures for both spin-up and spin-down polarization and without spin (SrSnO3) with GGA and mBJ–GGA approximations and in direction of Brillouin zone (BZ) for cubic structure

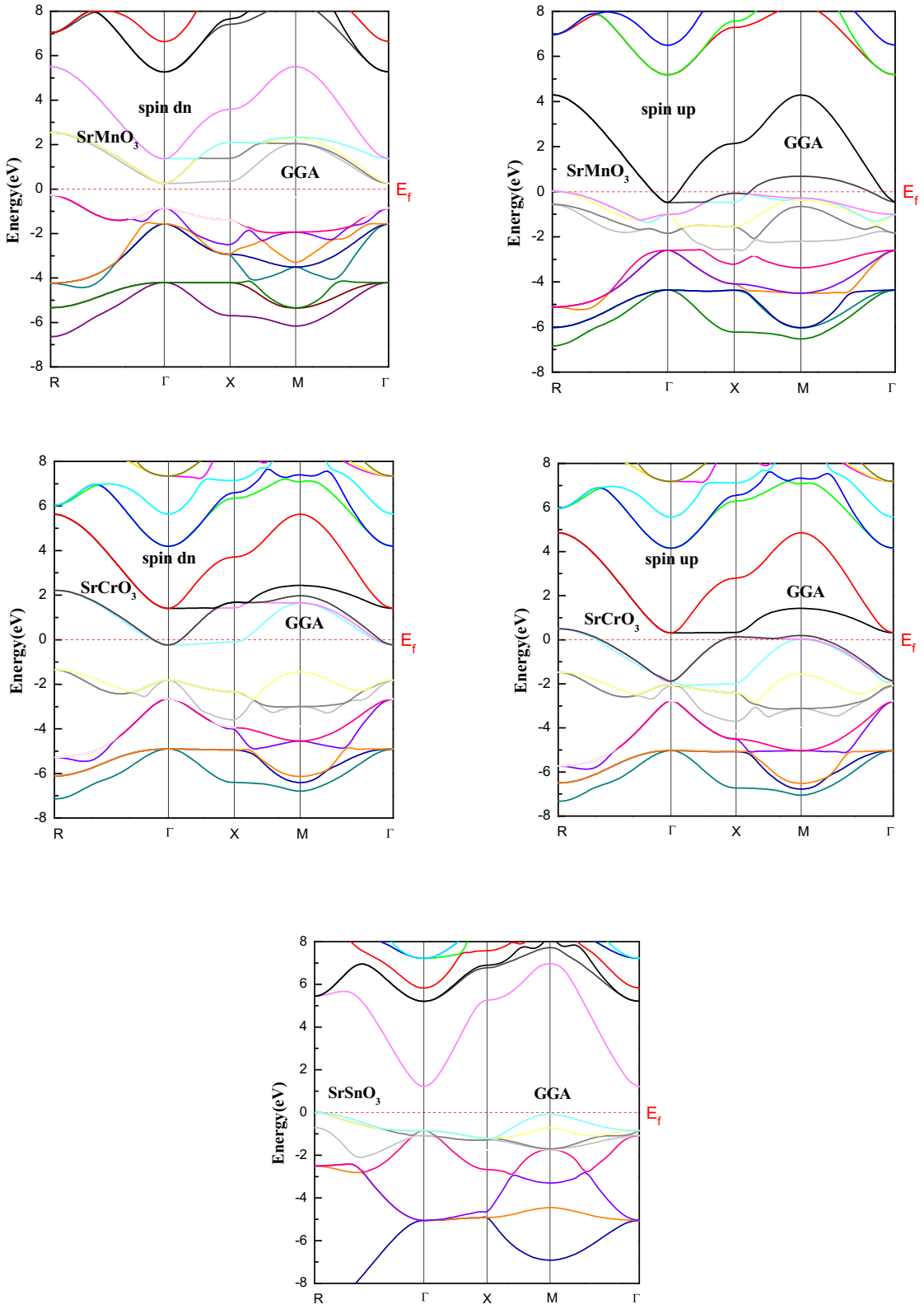

Fig. 3 Electronic bands structure for the perovskites $SrMnO_3$, $SrCrO_3$, and $SrSnO_3$ using the GGA approximation

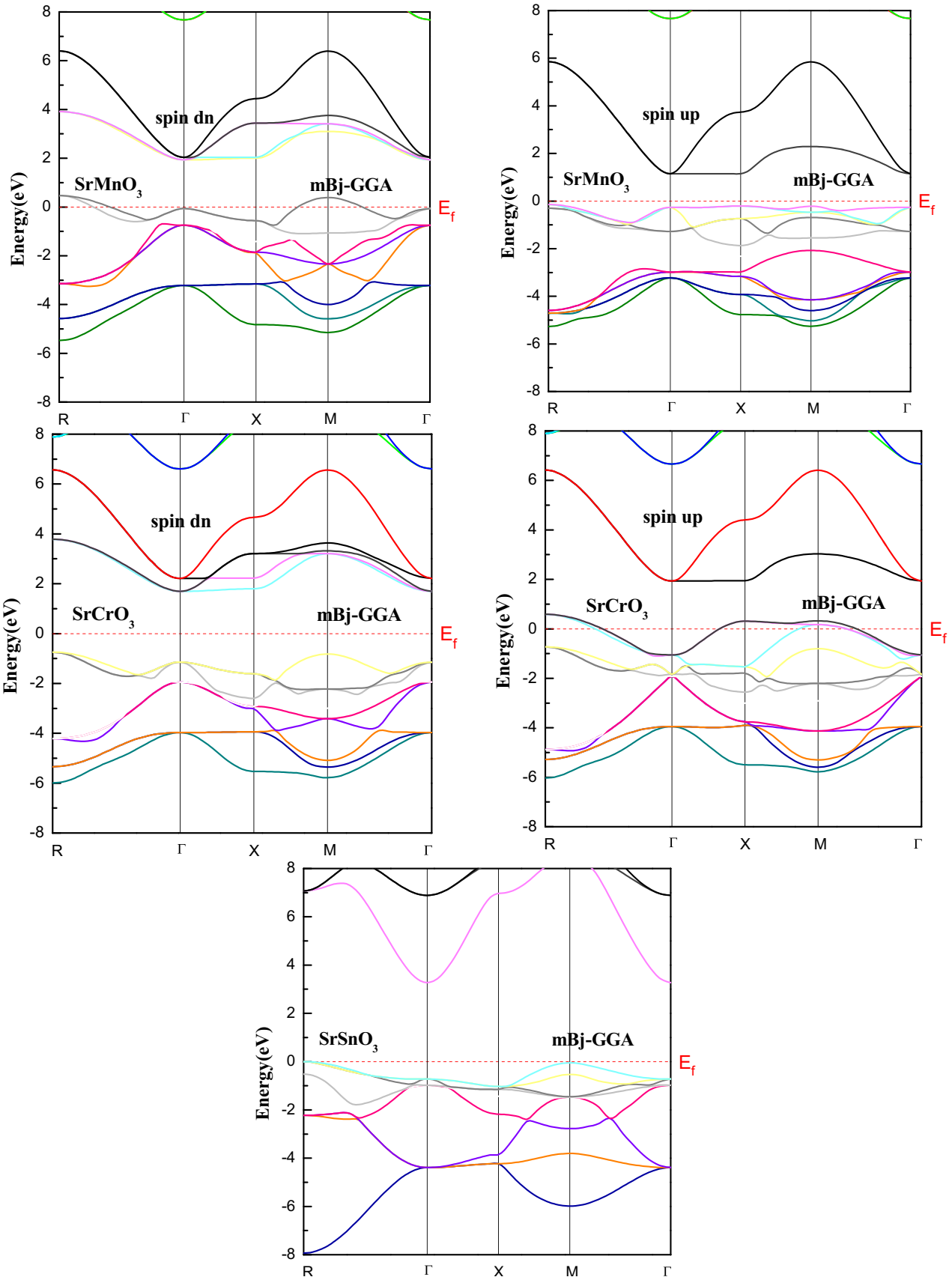

Fig. 4 Electronic bands structure for the perovskites $SrMnO_3$, $SrCrO_3$, and $SrSnO_3$ using the mBJ–GGA approximation

with high symmetry path (R-Γ-X-M-Γ). In these plots, the Fermi level is illustrated by a horizontal dash line and set to 0 eV to taken as an energy reference where the vertical axis, which ranged between − 8.0 and + 8.0 eV, represents the energy E (eV) of states relative to the Fermi energy. Every material has different electronic properties due to its unique band structures, so, starting by Fig. 3, our calculations show that the $SrMnO_3$ have a metallic behavior in the majority spin according to the few bands crossing the Fermi level and also have a semi-conductor behavior in the minority spin due to the energy gap that exists between the conduction and valence band which makes our SrMnO3 a half metallic perovskite. Here, in spin down, the valence band maximum is located at Γ with an energy of − 0.85196 eV and the conduction band minimum is at Γ with an energy equal to 0.25416 eV, so they are resulting in direct band gap equal to 1.10612 eV. For the $SrCrO_3$, it is clear from the bands crossing the E_F in both spin-up and spin-down channels that the perovskite is conductor material, and in spin down, the maximum energy values of the valence bands were − 1.8134 and 1.44757 eV, whereas the minimum energy values of the conduction bands were − 0.23933 and − 0.11353eV. While in spin up, the maximum energy values of the valence bands were 0.1314 and 0.1943 eV, and the minimum energy values of the conduction bands were 0.30856 and 0.32655 eV. These values indicate a larger overlap between the two bands. Therefore, there is no band gap. And our results show that the non-magnetic perovskite $SrSnO_3$ exhibit a semi-conducting nature due to the absence of the bands at the Fermi level and the clear band gap that located between the minimum of the conduction band Γ (1.21935 eV) and the maximum of the valence band M (− 0.07149 eV) with an energy equal to 1.29084 eV. This value is acceptable after comparing it with work of SHI Li-Wei et al. [32].

The outcomes of the electronic band structures using the mBJ–GGA approximation are shown in Fig. 4. For these computations, the Modified Becke–Johnson (mBJ) exchange potential is used for the enhancement of the band gap and the electronic properties of our materials. For the $SrMnO_3$ it can be clearly seen that our material is still a half metal but with a change between the spin-up and spin-down channels, and it exhibits a metal behavior at the spin-down configuration and the spin-up configuration shows the semi-conductor behavior where the conduction band bottom is at the Γ point with 1.14349 eV and the valence band top at the X point with − 0.20685 eV making an indirect band gap equal to 1.35034 eV and little larger than the previous one that obtained from the GGA approximation. We have changes too for the $SrCrO_3$ perovskites, the GGA approximations found it as a metallic material, but the mBJ–GGA approximation indicates that our $SrCrO_3$ is a half-metal perovskite; where we notice that the metallic character is kept in the majority spin due to the presence of some bands at the Fermi level, and a semi-conductor behavior appears at the minority spin configuration by the presence of a band gap between the CB and the VB. Remarking that the valence band maximum is located at M with an energy of − 0.82404 eV and the conduction band minimum at Γ with an energy equal to 1.69509 eV, they both make an indirect band gap equal to 2.51913eV. This is an important search as it differentiates the $SrCrO_3$ from the other perovskites. The same thing was achieved by S. Satapathy et al. in their research on Structural, Thermoelectric, and Magnetic Properties of Cubic $CdCrO_3$ [37], the nature of $CdCrO_3$ changed from a conductor to a semiconductor by adding the Coulomb repulsion terms GGA + U approximation as a correction to the GGA–PBE. Finally, the non-magnetic perovskite $SrSnO_3$ is still preserving its nature with a slight variation in the peaks which leads to the increase in the value of the band gap from 1.29084 eV to 3.27267eV in the same direction Γ-M (3.27267–0 eV). All of this difference between the three perovskites depends only on the X atom (X = Mn, Cr and Sn). The potential used as explained previously gave the most improved calculations, but there is no theoretical or experimental previous works to compare the band gap with. Also, this approximation shown that the two studied compounds ($SrMnO_3$ and $SrCrO_3$) are half metals in nature except $SrSnO_3$ which is semi-conductor material with the feature of n-type aspect.

To explain these behaviors, and contribution of different orbitals to the energy band structures especially for the band gaps found, we studied their total density (TDOS) and partial density of states (PDOS) to analyze the contribution of each atom in the electronic configuration of the system. Figures 5 and 6 show the total and partial density of states (TDOS and PDOS) of our studied cubic perovskites $SrXO_3$(X = Mn, Cr, and Sn), and the Fermi level (vertical red straight line) is positioned at zero energy ($E_F = 0.0$ eV). These results were obtained using both GGA and mBJ–GGA approximations with high spin-up and spin-down polarization and without spin polarization for only the $SrSnO_3$. TDOS proves our previous comment about the nature of our materials, and also, the mBJ–GGA approximation did a great job of correcting the results of the previous property and proved that the $SrMnO_3$ and the $SrCrO_3$ are half-metal perovskites; these calculated results indicate that the GGA–PBE functional have a little influence on the band-gap calculation. From their DOS plots, the electronic density for each compound is different in spin-up and spin-down states, demonstrating the magnetic nature, while the in the $SrSnO_3$ valence band, a higher density of

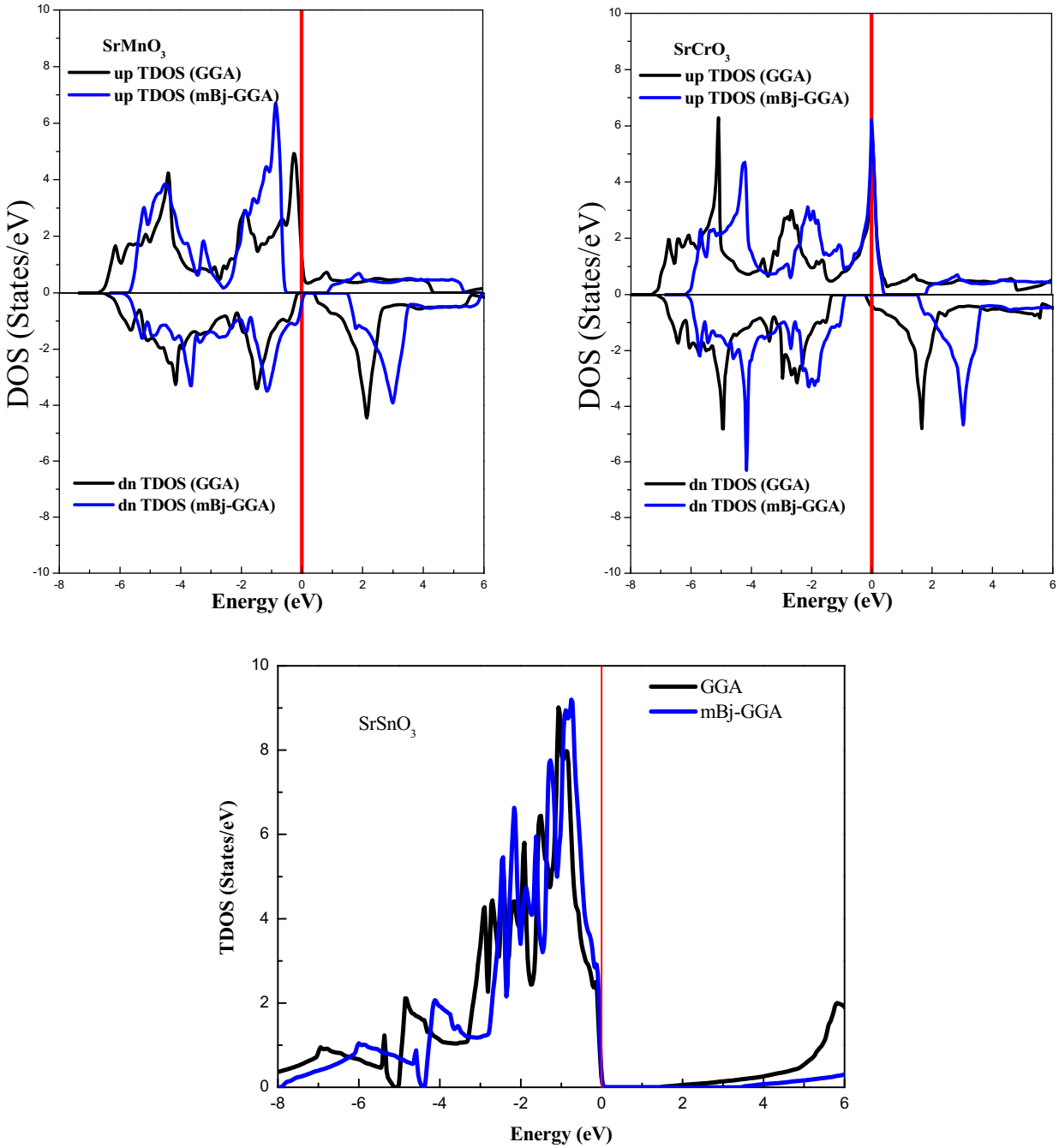

Fig. 5 Calculated total density of states TDOS for the perovskites $SrMnO_3$, $SrCrO_3$, and $SrSnO_3$ using both of the GGA and the mBJ–GGA approximations

states can be found, indicating that the structure belongs to the family of semi-conductors. To provide a more insight about the total DOS near the Fermi level; the partial DOS are also studied and shown in Fig. 6. Figure 6 shows the partial DOS of Sr, Mn, Cr, Sn, and O atoms for different s, p, and d orbitals. It is obvious from our results that the density of states of all studied compounds is divided into two parts; conduction and valence bands, and each one of theme is dominated by one, two, or all of the s, p, and d orbitals as presented in Fig. 6. For the $SrMnO_3$ the states

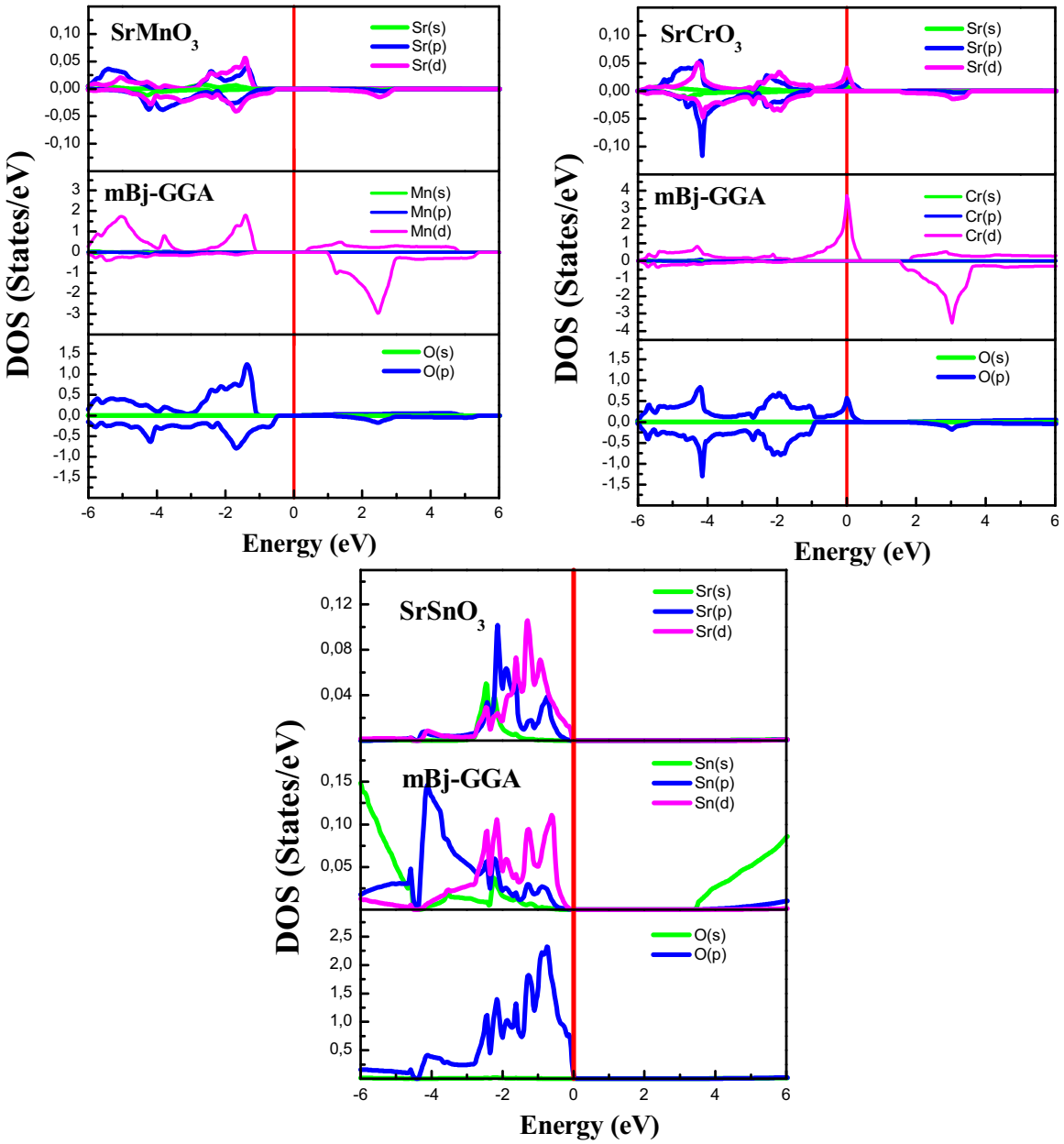

Fig. 6 Calculated partial density of states PDOS for the perovskites $SrMnO_3$, $SrCrO_3$, and $SrSnO_3$ using the mBJ–GGA approximation

beyond the E_F, from − 6 to − 1 eV, are mostly from the O (2p) and the Mn(3d) orbitals, whereas the conduction states close to EF, from + 0.5 to + 6 eV, are contributed by only the Mn (3d) orbitals. Generally, the two compounds show similar features, same notes for the $SrCrO_3$, the electronic properties here depend on the d−p hybridization between the Cr(d) and the O(p) atoms at the valence band from − 6eV to 0eV. Therefore, the p orbitals of Oxygen with strong electron occupations and the hybridization of d orbitals of X atom (X = Mn, Cr) are the main responsible of the half-metal aspect which appeared in those two compounds with an energy gap. And the PDOSs' curves of $SrSnO_3$ show that the heavy valence band of this material is essentially dominated by the O atom orbitals located at -6 and − 0.5 eV below the Fermi level, and in this region, the effect of the hybridization is weak for the p and d orbitals from the Sr and Sn atoms. The value of Eg increases

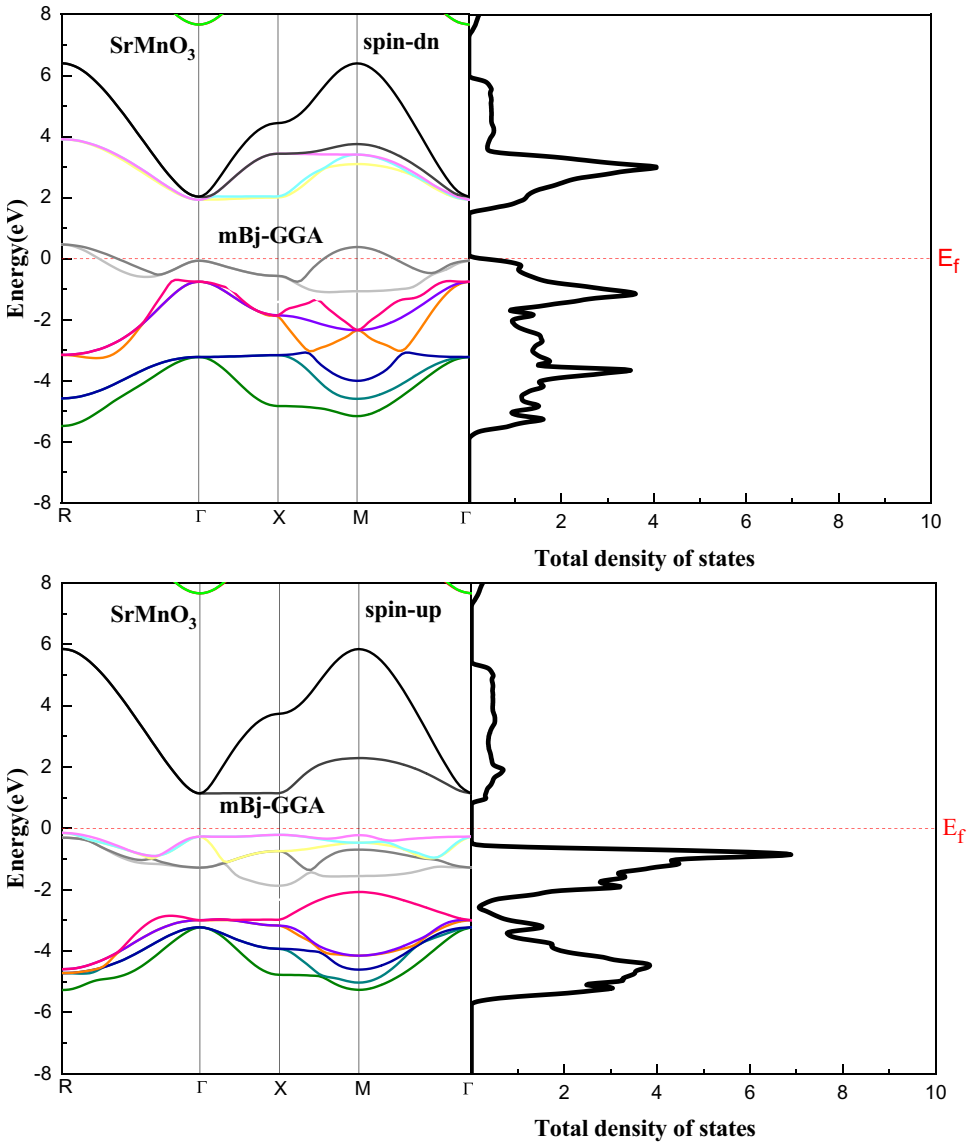

Fig. 7 Projection of the TDOS and BS for the magnetic perovskite $SrMnO_3$ using the mBJ–GGA approximation

linearly with the increase in electrons that occupy the X (3d) orbitals; Eg ($SrMnO_3$)< Eg ($SrCrO_3$)< Eg ($SrSnO_3$).

To demonstrate the correctness and the accuracy of our work of SC and HM properties and to elucidate details of the electronic structures of $SrXO_3$ (X = Mn, and Sn), we have plotted the projection between both of the total density of state and band structure using the mBJ–GGA approximation. The results are shown in Figs. 7, 8, 9. Based on the computed results, we expect positive industrial applications in spintronic and magnetic storage devices for the $SrMnO_3$ and the $SrCrO_3$ that depend mainly on the magnetic and electronic structures of the investigated compounds. On the other hand, the semi-conductor $SrSnO_3$ is very useful material to fabricate solar cells, light-emitting diodes (LEDs), photodetectors, lasers, X-ray scintillators, etc.

3.3 Magnetic properties

The transition metal strontium and chromate are responsible for the magnetic nature of those two perovskites. In this regard, we calculated the total and partial magnetic moments of the materials. The results are listed in Table 3.

It can totally see that the total magnetic moment of the $SrMnO_3$ is larger than the $SrCrO_3$ and that is due to the strong magnetism of the Mn atom; on the other hand, these two total magnetic moments' contributions are due to the Mn and Cr atoms in $SrMnO_3$ and $SrCrO_3$, respectively. While smaller negative values were observed for the Sr atom in both compounds after applying the mBJ–GGA approximation.

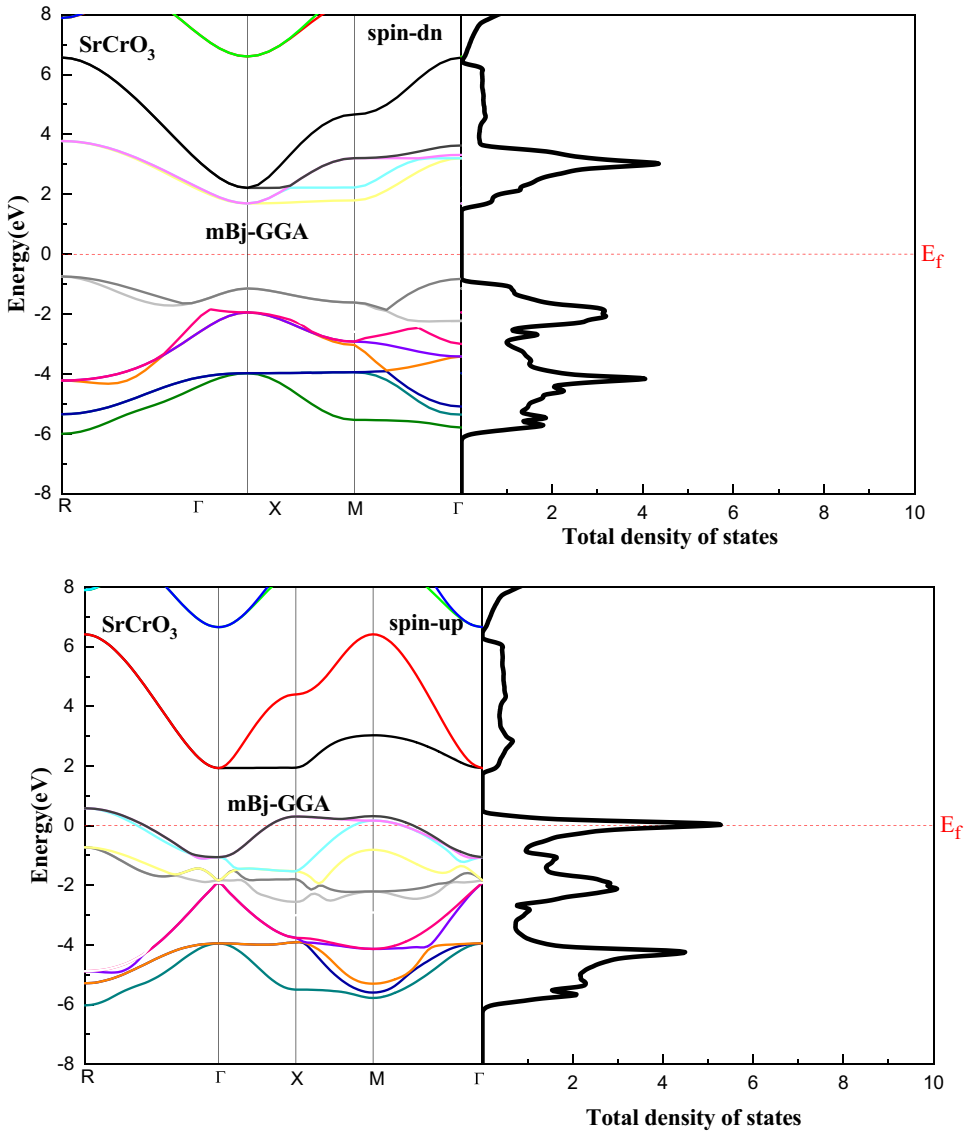

Fig. 8 Projection of the TDOS and BS for the magnetic perovskite $SrCrO_3$ using the mBJ–GGA approximation

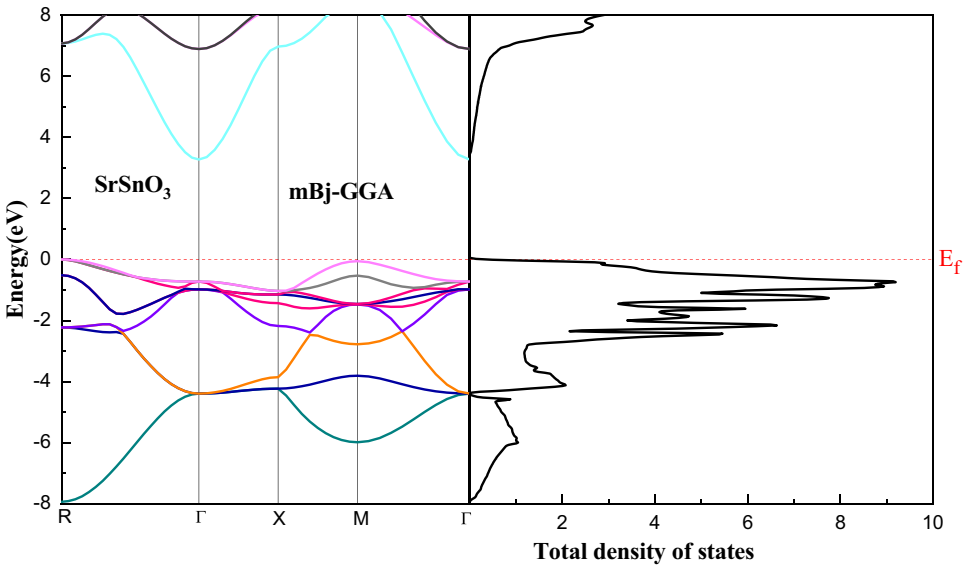

Fig. 9 Projection of the TDOS and BS for the non-magnetic perovskite $SrSnO_3$ using the mBJ–GGA approximation

Table 3 Calculated spin magnetic moments Mtotal (μB), partial spin magnetic moment M_{Sr} (μB), M_{Mn} (μB), and M_O (μB) for SrMnO3 with GGA-08 and mBJ–GGA functionals for SrMnO3 and SrCrO3

	Approximation	M_{total} (μ_B)	M_{Sr} (μ_B)	$M_{Mn/Cr}$ (μ_B)	M_O (μ_B)
This work	GGA–PBE	2.97821	0.01341	2.45870	0.08443
$SrMnO_3$	mBJ–GGA	3.00086	− 0.00195	2.55414	0.11801
EXP	–	3.6688 [38]	–	–	–
Other Calculation [36]	GGA–PBE	3.12854	0.00719	2.68818	0.07434
This work	GGA–PBE	1.94110	0.00063	1.60378	0.03281
$SrCrO_3$	mBJ–GGA	1.99999	– 0.00113	1.81169	0.00216
EXP	–	–	–	–	–
Other Calculation	–	–	–	–	–

4 Conclusion

In summary, we have employed the full-potential linearized augmented plane-wave (FPLAPW) approach based on density-functional theory implemented in wien2K code, within the generalized gradient approximation (GGA) and the mBJ–GGA functional, to study of structural, electronic, and magnetic properties of $SrXO_3$ (X = Mn, Cr, and Sn) compounds. The ground-state properties, including lattice constants, bulk modulus, and the total energies and the total and partial magnetic moments, were calculated and compared with the available theoretical and experimental previous works. The band structures and the partial contribution from each atom to the total density of states were also calculated. We observed that both of the $SrMnO_3$ and the $SrCrO_3$ perovskites had similar lattice parameter values. Therefore, where the $SrSnO_3$ is a non-magnetic semi-conductor with indirect (Γ-M) band gap. Moreover, $SrMnO_3$ and $SrCrO_3$ both were ferromagnetic semi-conductors with indirect (Γ-X) and (M-Γ) band gaps, respectively. And to complete the fundamental characteristics of those two half metals, we have calculated their magnetic properties. We believe that our study will encourage experimental efforts and inspire further studies of those compounds.

Funding No funding.

Data availability Not applicable.

Declarations

Conflict of interest No conflict interests.

References

1. S. Wang, X. Wang, L. Yuan, G. Ma, J. Zhang, Y. Zhang, X. Cui, X. Wu, D. Lu, Cryst. Growth Des. **20**(4), 2123–2128 (2020)
2. B. Sabir, G. Murtaza, R.A. Khalil, Q. Mahmood, J. Mol. Graph. Model. **86**, 19–26 (2019)
3. M.M. Hossain, A. AlMahmud, Comput. Condens. Matter **32**, e00695 (2022)
4. A.A. Adewale, A. Chik, R.M. Zaki, F. Che Pa, Y.C. Keat, N.H. Jamil, Solid State Phenom. **280**, 3–8 (2018)
5. Y. Selmani, H. Labrim, M. Mouatassime, L. Bahmad, Mater. Sci. Semicond. Process. **152**, 107053 (2022)
6. S. Idrissi, O. Mounkachi, L. Bahmad, A. Benyoussef, J. Korean Ceram. Soc. **60**, 424–433 (2023)
7. S. Idrissi, O. Mounkachi, L. Bahmad, A. Benyoussef, Comput. Condens. Matter **33**, e00617 (2022)
8. H. Labrim, Y. Selmani et al., Solid State Commun. **363**, 115105 (2023)
9. L. Xu, Z. Wang, B. Su, C. Wang, X. Yang, R. Su, X. Long, C. He, Crystals **10**, 434 (2020)
10. S. Idrissi, H. Labrim et al., J. Supercond. Nov. Magn. **34**, 2371–2380 (2021)
11. K. Kobayashi, D. Kan, S. Matsumoto, M. Mizumaki, Y. Shimakawa, J. Phys. Soc. Jpn. **88**, 084708 (2019)
12. H. Fu, R.E. Cohen, Nature **403**, 281–283 (2000)
13. U. Qazi, S. Mehmood, Z. Ali, I. Khan, I. Ahmad, Phys. B Condens. Matter **624**, 413361 (2022)
14. R.B. Behram, M.A. Iqbal, M. Rashid, M.A. Sattar, A. Mahmood, S.M. Ramay, Chin. Phys. B **26**, 116103 (2017)
15. K. Schwarz, P. Blaha, G.K.H. Madsen, Comput. Phys. Commun. **147**, 71 (2002)
16. R.M. Dreizler, E.K.U. Gross, *Density functional theory* (Springer, 1990)
17. G. Robert Parr, Y. Weitao, *Density-functional theory of atoms and molecules* (Oxford University Press, 1994)
18. P. Blaha, K. Schwarz, G.K.H. Madsen et al., *WIEN2k, an augmented plane wave plus local orbitals program for calculating crystal properties* (Vienna University of Technology, Vienna, 2001)
19. A.V. Nemtsev, V.S. Zhandun, V.I. Zineko, J. Exp. Theor. Phys. **126**, 497–505 (2018)
20. E. Cortés-Adasme, R. Castillo, S. Conejeros, M. Vega, J. Llanos, J. Alloys Compd. **771**, 162–168 (2018)
21. S. Tariq, A.A. Mubarak et al., Chin. J. Phys. **63**, 84–91 (2020)
22. J.P. Perdew, A. Ruzsinszky, G.I. Csonka, O.A. Vydrov, G.E. Scuseria, L.A. Constantin, X. Zhou, K. Burke, Phys. Rev. Lett. **100**, 136406–136414 (2008)
23. W. Kohn, L.J. Sham, Phys. Rev. **140**(4A), A1133–A1138 (1965)
24. F. Tran, P. Blaha, Phys. Rev. Lett. **102**, 226401 (2009)
25. F. Tran, P. Blaha, K. Schwarz, J. Phys. Condens. Matter **19**, 196208 (2007)
26. J.L. Erskine, E.A. Stern, Phys. Rev. Lett. **30**, 1329 (1973)
27. A. Kumar, M. Kumar, R.P. Singh, P.K. Singh, Solid State Commun. **324**, 114139 (2021)

28. S. Tariq, A.A. Mubarak, B. Kanwal, F. Hamioud, Q. Afzal, S. Zahra, Chin. J. Phys.. **63**, 84–91 (2020)
29. V.V. Bannikov, I.R. Shein, V.L. Kozhevnikov, A.L. Ivanovskii, J. Magn. Magn. Mater. **320**, 936 (2008)
30. F.D. Murnaghan, Proc. Natl. Acad. Sci. U.S.A. **30**, 244 (1944)
31. M. Musa, H.E. Saad, Bull. Mater. Sci. **44**, 171 (2021)
32. S. Li-Wei, D. Yi-Feng, Y. Xian-Qing, Q. Li-Xia, Chin. Phys. Lett. **27**, 096201 (2010)
33. O. Parkash et al., J. Mater. Sci. Lett. **13**, 1616 (1994)
34. R. Sondena, P. Ravindran, S. Stolen, T. Grande, M. Hanfland, Phys. Rev. B **74**, 144102 (2006)
35. L.O. San-Martin, A.J. Williams, J. Rodgers, J.P. Attfield, G. Heymann, H. Huppertz, Phys. Rev. Lett. **99**, 255701 (2007)
36. A. Kumar, M. Kumar et al., Solid State Commun. **324**, 114139 (2021)
37. S. Satapathy, M. Batouche, T. Seddik, M.M. Salah, K.K. Maurya, Crystals **13**, 1185 (2023)
38. M. Musa, H.E. Saad, J. Sci Adv Mater dev **2**, 115–122 (2017)